Inhibition of Ca^{2+} Sparks by Ruthenium Red in Permeabilized Rat Ventricular Myocytes

Valeriy Lukyanenko,* Inna Györke,* Saisunder Subramanian,† Anton Smirnov,* Theodore F. Wiesner,† and Sandor Györke*

*Department of Physiology, Texas Tech University Health Sciences Center, Lubbock, Texas 79430, and †Department of Chemical Engineering, Texas Tech University, Lubbock, Texas 79409-3121 USA

ABSTRACT We have compared the effects of the sarcoplasmic reticulum (SR) Ca^{2+} release inhibitor, ruthenium red (RR), on single ryanodine receptor (RyR) channels in lipid bilayers, and on Ca^{2+} sparks in permeabilized rat ventricular myocytes. Ruthenium red at 5 μM inhibited the open probability (P_o) of RyRs ~20–50-fold, without significantly affecting the conductance or mean open time of the channel. At the same concentration, RR inhibited the frequency of Ca^{2+} sparks in permeabilized myocytes by ~10-fold, and reduced the amplitude of large amplitude events (with most probable localization on the line scan) by ~3-fold. According to our theoretical simulations, performed with a numerical model of Ca^{2+} spark formation, this reduction in Ca^{2+} spark amplitude corresponds to an ~4-fold decrease in Ca^{2+} release flux underlying Ca^{2+} sparks. Ruthenium red (5 μM) increased the SR Ca^{2+} content by ~2-fold (from 151 to 312 μmol/l cytosol). Considering the degree of inhibition of local Ca^{2+} release events, the increase in SR Ca^{2+} load by RR, and the lack of effects of RR on single RyR open time and conductance, we have estimated that Ca^{2+} sparks under normal conditions are generated by openings of at least 10 single RyRs.

INTRODUCTION

In cardiac muscle the process of excitation-contraction coupling is mediated by Ca^{2+} influx through voltage-dependent Ca^{2+} channels, which activate Ca^{2+} sensitive Ca^{2+} release channels in the membrane of the sarcoplasmic reticulum (SR) (Bers, 1991; Cheng et al., 1996; Overend et al., 1998; Bers and Perez-Reyes, 1999). The global Ca^{2+} release during excitation-contraction (E-C) coupling appears to be a result of the summation of microscopic Ca^{2+} release events called Ca^{2+} sparks (Cheng et al., 1993; Cannell et al., 1994; Lopez-Lopez et al., 1995). Although it is becoming increasingly clear that Ca^{2+} sparks represent elementary release events of E-C coupling, their functional organization, in particular whether they are due to activation of a single ryanodine receptor (RyR) or the concerted opening of many RyRs, remains controversial. Ultrastructural evidence reveals that ~22 release channels are present in a typical SR junctional cleft (Franzini-Armstrong and Protasi, 1997). Mathematical modeling suggests that a Ca^{2+} influx of 10 mM/s (which is similar to Ca^{2+} flux associated with a spark (Blatter et al., 1997; Lukyanenko et al., 1998)) into the narrow junctional cleft can increase local free [Ca^{2+}] up to levels of 100–600 μM (Langer and Peskoff, 1996). It would be reasonable to assume that, at these Ca^{2+} concentrations, all or most of the Ca^{2+} channels in the cleft become activated. The multi-channel origin of sparks is also supported by the multi-focal structure of release events in confocal images (Parker et al., 1996; Blatter et al., 1997). In addition, it has been shown that Ca^{2+} release induced by photolysis of caged Ca^{2+} is spatially homogeneous, suggesting elementary release events smaller than Ca^{2+} sparks (Lipp and Niggli, 1996). In contrast, the single channel interpretation of sparks would be consistent with the small amplitude of the release flux relative to the expected Ca^{2+} conductance of single RyRs, and by the apparent similarities between the action of ryanodine and FK506 on spark behavior and single channel gating (Cheng et al., 1993; Xiao et al., 1997). Furthermore, it has been demonstrated that depletion of SR Ca^{2+} has no significant impact on the frequency of spontaneous Ca^{2+} sparks, which would be consistent with Ca^{2+} sparks representing single openings of channels that are not influenced by unitary Ca^{2+} flux (Song et al., 1997). In this study we have probed the functional organization of release units by correlating the effects of the Ca^{2+} release channel blocker ruthenium red (RR) on single RyRs and Ca^{2+} sparks. If the release units underlying Ca^{2+} sparks are composed of multiple channels, then it should be possible to decrease the amplitude of the sparks by RR. The degree of inhibition of the signal could potentially provide information on the number of channels involved in a release unit.

MATERIALS AND METHODS

Confocal microscope

Single ventricular myocytes were obtained from adult male Sprague-Dawley rat hearts by enzymatic dissociation as described previously (Györke et al., 1997). The animals were killed by lethal injection of Nembutal (100 mg/kg i.p.). The standard Tyrode's solution contained (in mM): 140 NaCl, 5.4 KCl, 0.5 $MgCl_2$, 1 $CaCl_2$, 10 Hepes, 0.25 NaH_2PO_4, 5.6 glucose, pH 7.3. The cells were permeabilized by exposure to saponin (0.01% for 45–60 s, Lukyanenko and Györke, 1999). The permeabilization solution contained (in mM): 120 potassium aspartate, 3 MgATP (free [Mg^{2+}] ~1 mM), 0.5 EGTA, 10 phosphocreatine, 5 U/ml creatine phosphokinase, and 8% dextran (40,000, to prevent osmotic swelling of the cells), pH 7.2. The control experimental solution contained (in mM): 120

Received for publication 27 January 2000 and in final form 31 May 2000.

Address reprint requests to Dr. Sandor Györke, Department of Physiology, Texas Tech University HSC, 3601 4th St., Lubbock, TX 79430. Tel.: 806-743-2520; Fax: 806-743-1512; E-mail: physg@ttuhsc.edu.

0006-3495/00/09/1273/12 $2.00

potassium aspartate, 3 MgATP, 0.5 EGTA, 0.114 $CaCl_2$ (free $[Ca^{2+}]$ ~100 nM), 10 phosphocreatine, 0.03 Fluo-3 K-salt (TefLabs, Austin, TX) and 5 U/ml creatine phosphokinase, pH 7.2. The free $[Ca^{2+}]$ at given total Ca^{2+}, Mg^{2+}, ATP, and EGTA concentrations were calculated using a computer program (WinMAXC 1.80, Stanford University, CA). Ca^{2+} sparks and caffeine-induced Ca^{2+} transients were recorded by using a Bio-Rad Laser Scanning Confocal system (MRC 1024ES, Bio-Rad Laboratories, Hercules, CA) equipped with an Olympus 60 × 1.4 N.A. objective. Fluo-3 was excited by light at 488 nm (25 mW argon laser, intensity attenuated to 0.3–1%), and fluorescence was measured at wavelengths of >515 nm. An analog recording of fluorescence intensity during each scan was digitized into 768 or 1024 pixels, giving a nominal pixel dimension of 0.33 or 0.24 μm. Images were acquired at a rate of 2.0 ms per scan. Fluorescence $F(x_i, t)$ was normalized to its basal average F_0, and presented as F/F_0 or $\Delta F/F_0$, where $\Delta F = F_{peak} - F_0$. The basal average F_0 for the ith column was computed using IDL software (Research Systems Inc., Boulder, CO) after excising the pixels that were more than three times higher in amplitude than a mean standard deviation for the column. Each element of the ith column was then divided by its respective column average, yielding a self-ratioed image.

Ca^{2+} sparks were quantified using a detection computer algorithm (Cheng et al., 1999; Lukyanenko and Györke, 1999). To exclude false events, the threshold for event detection was set so that no events would be identified under conditions when the SR Ca^{2+} release was abolished by exposing the cells to ryanodine (10 μM) and thapsigargin (10 μM). The frequency and amplitude ($\Delta F/F_0$) of events were corrected for detectability and amplitude distortions introduced by instrumental noise as described elsewhere (Song et al., 1997). Test images were generated by scaling the intensity of an averaged Ca^{2+} spark obtained from 28 individual events to various levels and contaminating the signals by random Gaussian noise at a level similar to that in experimental images. The test images were fed to our computer algorithm to evaluate the performance of the program and to generate correction curves for frequency and amplitude of events. The correction functions for frequency and amplitude are presented in Fig. 1.

The SR Ca^{2+} content under control conditions and in the presence of RR was determined from the peak amplitude of the Ca^{2+} transients induced by application to the permeabilized cells of 20 mM caffeine (Kawai and Konishi, 1994; Bassani et al., 1995). Free calcium ($[Ca^{2+}]_f$) changes were calculated from fluo-3 fluorescence using Eq. 1.

$$[Ca^{2+}]_f = K_{fluo}R/(K_{fluo}/[Ca^{2+}]_{rest} - R + 1) \quad (1)$$

where $R = F/F_0$ and $[Ca^{2+}]_{rest}$ is the free $[Ca^{2+}]$ in the "internal" solution (adjusted to 100 nM) (Cannell et al., 1994). The change in $[Ca^{2+}]_f$ on caffeine application (peak $[Ca^{2+}]_f$ − basal $[Ca^{2+}]_f$) was converted into a change in total calcium (peak $[Ca^{2+}]_t$ − basal $[Ca^{2+}]_t$) using Eq. 2

$$[Ca^{2+}]_t = [Ca^{2+}]_f + \frac{[EGTA]}{\left(1 + \frac{K_{EGTA}}{[Ca^{2+}]_f}\right)} + \frac{[Troponin\text{-}C]}{\left(1 + \frac{K_{trop}}{[Ca^{2+}]_f}\right)} + \frac{[fluo\text{-}3]}{\left(1 + \frac{K_{fluo}}{[Ca^{2+}]_f}\right)} \quad (2)$$

where [EGTA] = 0.5 mM, K_{EGTA} = 163 nM, [fluo-3] = 30 μM, K_{fluo} = 740 nM, [Troponin-C] = 70 μM, and K_{trop} = 0.5 μM. This was considered the SR Ca^{2+} content at the time of caffeine application.

Lipid bilayer experiments

Heavy sarcoplasmic reticulum microsomes were prepared from the ventricles of dog heart using standard procedures (Dettbarn et al., 1994). Single RyRs were reconstituted by fusing SR microsomes into planar lipid bilayers as described previously (Györke et al., 1997; Györke and Györke, 1998). Channel incorporation was performed in solutions containing 350 mM $CsCH_3SO_3$, 20 μM $CaCl_2$, 20 mM Hepes (pH 7.2) on the cytosolic (*cis*) side of the bilayer, and 20 mM $CsCH_3SO_3$, 20 μM $CaCl_2$, 20 mM Hepes, (pH 7.2) on the lumenal (*trans*) side of the bilayer. The experimental solutions contained 350 mM $CsCH_3SO_3$, 20 or 305 μM $CaCl_2$ (free $[Ca^{2+}]$ ~2 μM or 100 μM, respectively), 3 mM MgATP, 300 μM $MgCl_2$, 20 mM Hepes, pH 7.2 (*cis*), and 20 or 350 mM $CsCH_3SO_3$, 20 μM or 1 mM $CaCl_2$, 20 mM Hepes, pH 7.2 (*trans*). Single channels were monitored either at +30 mV in symmetrical Cs^{2+} (350 mM) or at 0 mV in the

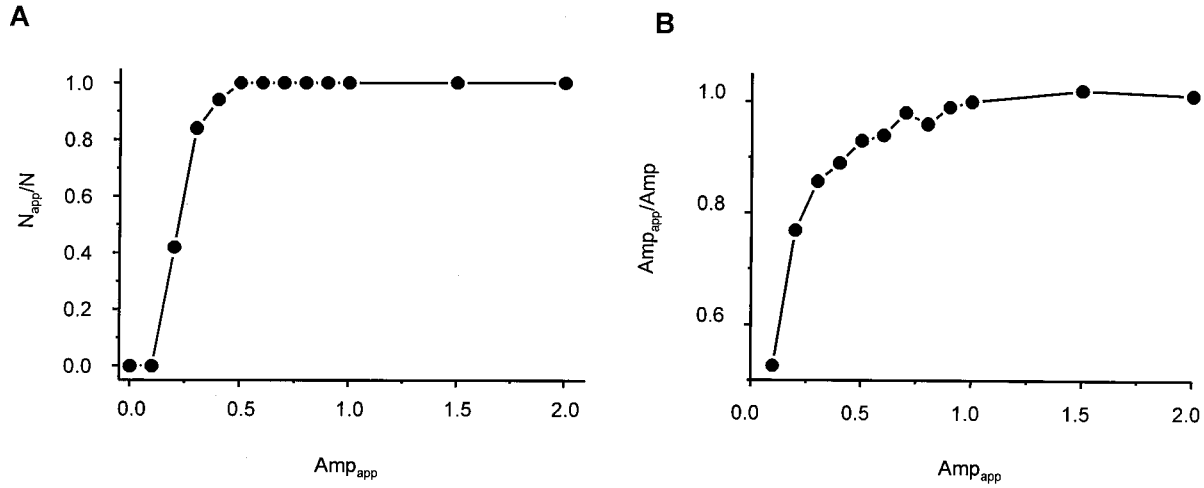

FIGURE 1 Frequency and amplitude correction functions for quantification of Ca^{2+} sparks. Relationships between the number (N_{app}, *A*) or amplitude (Amp_{app}, *B*) of Ca^{2+} sparks as reported by our spark detection program and the true number (*N*) or amplitude (Amp) values of Ca^{2+} sparks, respectively, for test images containing standard Ca^{2+} sparks of different fluorescence intensities. An average Ca^{2+} spark was constructed by superimposing 28 individual events; this spark was scaled to various intensity levels and contaminated with random Gaussian noise similar to that in experimental images. Each point was obtained by feeding 100 standard Ca^{2+} sparks to the computer algorithm.

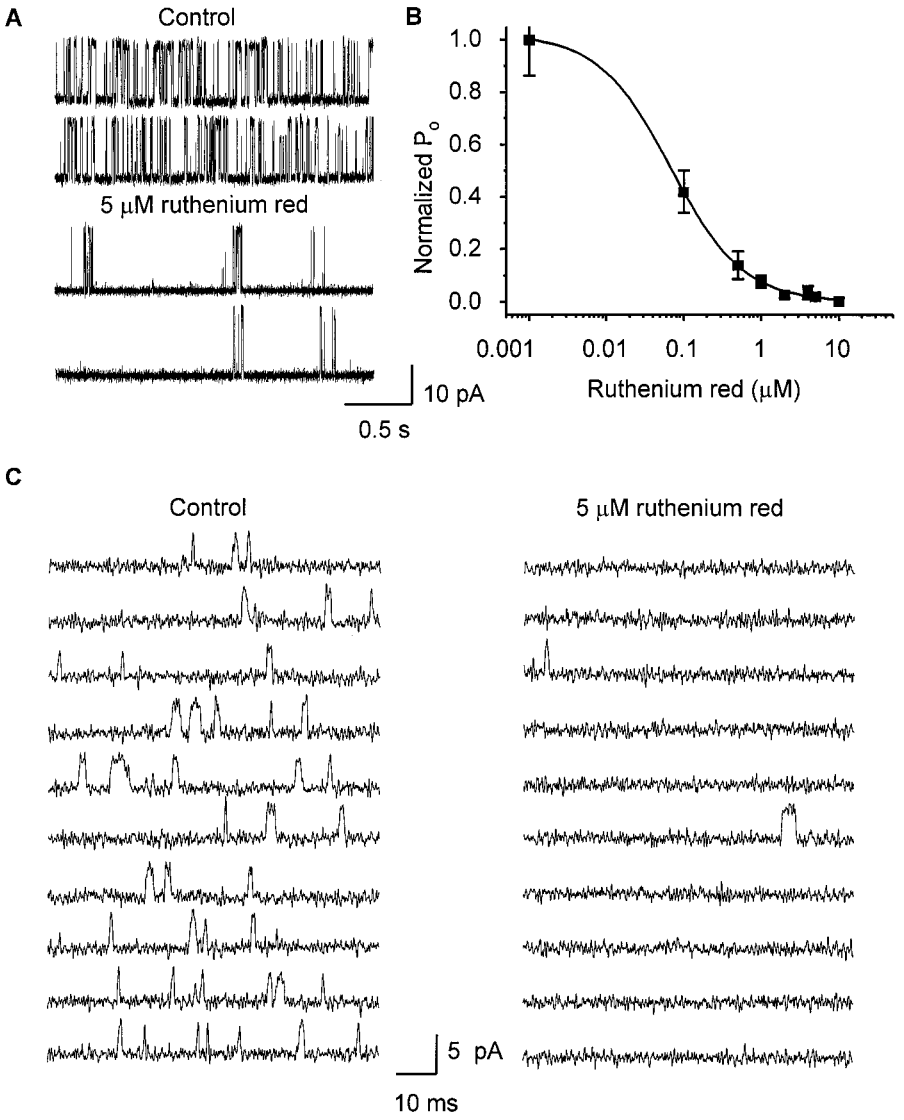

FIGURE 2 Inhibition of single cardiac RyRs by RR. (*A*) Representative single channel recordings performed in symmetrical Cs^+ under control conditions and in the presence of 5 μM RR. Channel openings are upward. Holding potential was +30 mV; *cis* [Ca^{2+}] was 100 μM; *trans* [Ca^{2+}] was 20 μM. (*B*) Dose-response relationship for inhibition of RyR channel P_o by RR under the same experimental conditions as in (*A*). Data are presented as mean ± SEM of 4–6 determinations from different experiments. The continuous curve was obtained by fitting the data according to the equation $P_o = 1/(1 + ([RR]/EC_{50})^p)$ with $EC_{50} = 0.07$ μM and $p = 0.93$. (*C*) Representative single channel recordings performed in the presence of a Cs^+ gradient (350 mM *cis*/30 mM *trans*) under control conditions and in the presence of 5 μM RR. Channel openings are upward. Holding potential was 0 mV; *cis* [Ca^{2+}] was 2 μM; *trans* [Ca^{2+}] was 1 mM.

presence of a Cs^{2+} gradient (350 mM *cis*/20 mM *trans*). Single channel currents were recorded with an Axopatch 200A (Axon Instruments, Foster City, CA) patch clamp amplifier. Data were filtered at 2–5 kHz and digitized at 5–10 kHz. Acquisition and analysis of data were performed using pClamp 6.01 software (Axon Instruments, Foster City, CA).

Generation of theoretical amplitude histograms for sources of various strength

Spherically symmetric spatiotemporal distributions of free calcium concentration, free indicator concentration, and the concentration of the calcium-indicator complex Ca:dye (*r, t*) were obtained by numerically solving the reaction-diffusion system described previously (Lukyanenko et al., 1999). The release flux was modeled as the exponentially decaying function given in Eq. 3.

$$q_{rel}(r, t) = \begin{cases} q_0 e^{-t/\tau} & r = \text{location of spark source} \\ 0 & \text{elsewhere} \end{cases} \quad (3)$$

The peak release flux q_0 varied from 2.4 to 12.5 mM/s. The decay constant τ was 2 ms for all simulations.

Images of Ca^{2+} sparks were generated by using the general approaches formulated by Pratusevich and Balke (1996) and Smith et al. (1998). Image formation by the confocal microscope was simulated by spatially convolving the calcium-dye concentration with a theoretical point spread function.

$$I(r, t) = \text{Ca:dye}(r, t) \cdot \text{PSF}(r) \quad (4)$$

The point spread function featured a Gaussian distribution

$$\text{PSF}(r) = \frac{1}{\sqrt{2\pi\sigma_r}} e^{-(r/\sigma_r)^2} \quad (5)$$

The standard deviation of the point spread function was taken as $\sigma_\gamma = 0.6$ μm for all simulations. The convolution was carried out in the Fourier domain using IDL software (Research Systems Inc., Boulder, CO).

To simulate scanning out-of-focus from the center of the spark, we randomly sampled the theoretical sparks at radii offset from the spark center. We used the Inversion Generating Method (Gillespie, 1976), in which a set of uniformly distributed random numbers is used to generate another set of random numbers distributed according to a prescribed probability density function. A spark spherically symmetric about the

release site presents a circular cross-section perpendicular to the direction of the line scan. Taking the spark radius R as the furthest extent of fluorescence from the source, the probability density of a scan at radius r from the spark center is $f(r) = 2r/R^2$. The probability distribution function corresponding to this density is $f(r) = (r/R)^2$. Inversion of this distribution function leads to Eq. 6.

$$r = R\sqrt{x} \tag{6}$$

Here r is the randomly distributed radius of offset and x is the uniformly distributed random number selected by Monte Carlo draw. Such a distribution is skewed toward the larger radii, leading to a set of sparks whose intensities are skewed toward lower amplitudes.

RESULTS

Effects of RR on single RyRs

Heavy cardiac SR microsomes were fused into planar lipid bilayers, and single RyR channels were monitored using Cs^+ as the charge carrier. The solutions on the cytosolic (*cis*) side of the channel contained 3 mM ATP and 3.3 mM Mg^{2+} (free [Mg^{2+}] ~1 mM) to match the concentration of these ions in the "internal" solutions in our permeabilized myocyte experiments (see below). The effects of RR on the activity of single RyR channels recorded at +30 mV in the presence of 100 μM *cis* [Ca^{2+}] are illustrated in Fig. 2, *A* and *B*. Panel *A* shows representative recordings of a single channel before and after addition (4 min) of the drug (5 μM), panel *B* presents the average dose-response relationship for the reduction of P_o by the drug. The half-maximal inhibition of P_o was near 0.1 μM; at 5 μM the drug inhibited P_o by ~98%. The effects of RR on RyR gating at three different concentrations (0.1, 1, and 5 μM) are summarized in Table 1. As can be seen, RR reduced the overall channel activity by decreasing the frequency of openings without significantly affecting the lifetimes of openings or amplitude of the currents.

The ability of RR to inhibit RyRs could potentially be influenced by the membrane potential. (The SR membrane is thought to maintain no voltage gradient (Baylor et al., 1984).) In addition, the effects of RR on RyR gating could depend on both cytosolic and lumenal Ca^{2+}. ([Ca^{2+}] in the dyadic cleft during a spark is believed to vary between 100 nM and 100 μM (Blatter et al., 1997), and $[Ca^{2+}]_{SR} \approx$ 1 mM (Bers, 1991).) To assess the potential impact of these factors on the inhibition of RyRs by the drug, we performed additional experiments with the membrane potential set to 0 and in the presence of 1 mM Ca^{2+} on the lumenal (*trans*) side of the bilayer. The *cis* [Ca^{2+}] in these experiments was adjusted to ~2 μM (the lowest concentration at which a sufficient number of events could be collected for analysis in the presence of the drug) to better correspond to cytosolic Ca^{2+} concentration at the onset of the Ca^{2+} sparks. Representative traces recorded under control conditions and after addition of 5 μM RR to the *cis* compartments are presented in Fig. 2 *C*. Exposure of the channels to 5 μM RR inhibited P_o by ~95% (from 0.0111 ± 0.0018 to 0.0005 ± 0.0002, $n = 3$). Again, the inhibition occurred without significant alterations in the mean open time (1.2 ± 0.1 ms vs. 0.9 ± 0.2 ms, $n = 3$) or single channel current (5.4 ± 0.1 pA vs. 5.2 ± 0.3 pA, $n = 3$). Thus it appears that the mechanism and extent of inhibition of RyR by RR are similar under a wide range of experimental conditions that are likely to cover the potential differences in the conditions of our bilayer versus permeabilized cell experiments.

Effects of RR on Ca^{2+} sparks

We investigated the effects of RR on spontaneous Ca^{2+} release events (Ca^{2+} sparks) in saponin-permeabilized myocytes. Permeabilization was performed using saponin in "internal" solutions containing 30 μM fluo-3 and 0.5 mM EGTA (pCa 7). We have demonstrated recently that under these conditions, permeabilization does not significantly alter the frequency and spatiotemporal characteristics of Ca^{2+} sparks (Lukyanenko and Györke, 1999). Application of RR (>1 μM) to the internal solution caused a reduction in the rate of occurrence and brightness of Ca^{2+} sparks. With submaximal blocking concentrations of 5–10 μM, the inhibition developed in the course of 3–5 min and remained steady for at least 10 min (not shown). At >10 μM, RR completely abolished sparking activity. To attain strong inhibition while retaining the ability to collect a sufficient number of events for analysis, most experiments were performed with 5 μM of RR.

Fig. 3 *A* illustrates representative line scan images obtained from a permeabilized myocyte under control conditions and after successive additions to the internal solution of 5 and 20 μM RR. Time-dependent profiles of the brightest Ca^{2+} sparks are also presented below the images. In accordance with our previous findings (Lukyanenko and Györke, 1999), permeabilized cells exhibited Ca^{2+} sparks

TABLE 1 Effect of ruthenium red on RyR properties

		Ruthenium Red Concentration		
Channel Properties	Control	0.1 μM	1 μM	5 μM
Open Probability (P_o)	0.225 ± 0.031	0.094 ± 0.018	0.017 ± 0.005	0.004 ± 0.002
Mean open time (ms)	0.84 ± 0.05	0.67 ± 0.14	0.56 ± 0.13	0.78 ± 0.21
Mean closed time (ms)	8 ± 3	58 ± 24	97 ± 39	3160 ± 2290

Data are presented as means ± SEM of 8–13 determinations from different experiments.

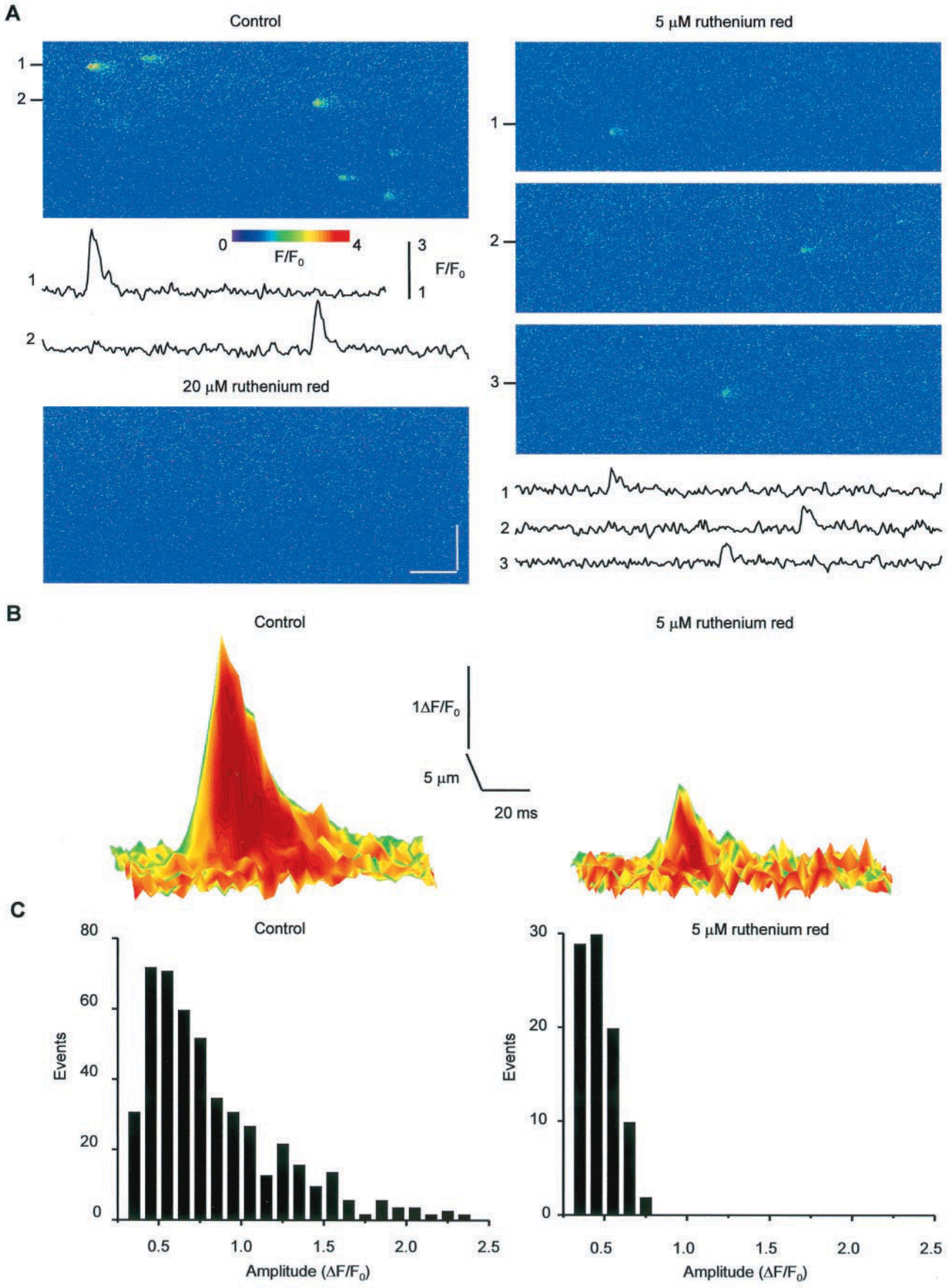
A
Control
5 μM ruthenium red
20 μM ruthenium red
1
2
3
0
4
F/F0
3
1
F/F0
B
Control
5 μM ruthenium red
1ΔF/F0
5 μm
20 ms
C
Control
5 μM ruthenium red
Events
Amplitude (ΔF/F0)
80
60
40
20
0
30
10
0.5
1.0
1.5
2.0
2.5

with a frequency of ~6 events/s/100 μm (6.36 $\pm$ 0.65, n = 43) and practically no spontaneous Ca^{2+} waves under control conditions. Incubation with 5 μM of RR caused an ~10-fold decrease in overall frequency of events (0.62 $\pm$ 0.14, n = 46). In addition, the brightness and the spatiotemporal size of the fluorescence events were reduced dramatically. In the presence of 20 μM RR, the cells exhibited no detectable local fluorescence signals.

Fig. 3 *B* illustrates the effects of RR on surface plots of averaged Ca^{2+} sparks constructed by superimposing 10 of the brightest events obtained under control conditions and 6 of the brightest events in the presence of RR. In the presence of the drug, the peak amplitude of the fluorescence signal is reduced by ~3-fold with respect to the control situation. At the same time, the width and duration (at half-maximal width) of the signal are reduced by 40% and 50%, respectively.

The amplitude histograms of the events measured using our automated event detection algorithm under control conditions and in the presence of the drug are shown in Fig. 3 *C*. The histograms were corrected for noise-related distortions in the frequency and amplitude of the events using test images that contained standard Ca^{2+} sparks with certain amplitudes (Song et al., 1997). As demonstrated previously (Song et al., 1997), the amplitude distribution of Ca^{2+} sparks is skewed to lower values by out-of-focus events. The small fractions of events on the high amplitude end of the graphs have the highest probability of being localized at the center of the line scan (Izu et al., 1998; see below). At 5 μM, RR dramatically reduced the number of large amplitude events (>0.5 $\Delta F/F_0$) narrowing the distribution, and shifting it toward the low amplitude end. The mean amplitude of Ca^{2+} sparks comprising 5% of the brightest events was inhibited 2.8-fold (1.95 $\pm$ 0.04, n = 23; vs. 0.70 $\pm$ 0.06, n = 5) by RR. At 20 μM, RR eliminated virtually all events. Similarly, no events were detected in cells in which the SR Ca^{2+} stores were depleted by a pretreatment with ryanodine (10 μM) and thapsigargin (10 μM; not shown). These experiments confirm that the events identified by our detection algorithm in the presence of 5 μM RR are related to Ca^{2+} release from the SR.

To further investigate whether the small events acquired in the presence of RR are associated with operation of RyRs, we carried out experiments using the specific agonists of RyRs, caffeine, and ryanodine. It is believed that caffeine can induce RyR channel openings by sensitizing the channels to cytosolic Ca^{2+}. Ryanodine at submicromolar concentrations appears to act by locking the RyR into a long-lived sub-conductance state (Meissner, 1994). Consistent with the effects of these compounds on RyRs, caffeine increased the frequency of the small-amplitude events in the presence of RR (from 0.76 $\pm$ 0.16 to 5.15 $\pm$ 0.37 events/s/100 μm, n = 5) while ryanodine increased their duration (from 16.4 $\pm$ 0.56 ms to 33.3 $\pm$ 3.43 ms, n = 35; Fig. 4, *A* and *B*, respectively). These effects occurred without significant changes in the magnitude of the events (0.55 $\pm$ 0.03 $\Delta F/F_0$, n = 38 vs. 0.53 $\pm$ 0.04 $\Delta F/F_0$, n = 31 in the presence of caffeine; and 0.54 $\pm$ 0.04 $\Delta F/F_0$, n = 31 vs. 0.56 $\pm$ 0.03 $\Delta F/F_0$, n = 32 in the presence of ryanodine). These results provide additional evidence that the small events in the presence of RR are caused by openings of RyR channels.

Effects of varying source strength on amplitude distribution of theoretical Ca^{2+} sparks

The Ca^{2+} spark is only a crude measure of the underlying Ca^{2+} source. It is corrupted by inaccuracies in image acquisition (i.e., optical distortion, scanning out-of-focus and instrumental noise) and by effects of various diffusion, transport, and binding processes (Pratusevich and Balke, 1996; Smith et al., 1998). To better understand the effects of RR on the RyR gating behavior underlying Ca^{2+} sparks, we have performed theoretical simulations using a numerical model of the Ca^{2+} spark. The mathematical model of Ca^{2+} spark formation, including the effects of the microscope, was constructed according to the approaches described previously (Pratusevich and Balke, 1996; Smith et al., 1998; Izu et al., 1998; see Methods). The peak Ca^{2+} flux underlying Ca^{2+} sparks has been estimated in the range of 2–10 mM/s (Blatter et al., 1997; Lukyanenko et al., 1998). We simulated Ca^{2+} sparks using underlying Ca^{2+} fluxes of 2.4, 6.0, 10.0, and 12.5 mM/s. The theoretical amplitude distributions were generated by randomly varying the scanning line position around the center of a standard spark. Our simulations do not include the effects of instrumental noise because the experimental data were corrected for distortion in frequency and amplitude of the events. Images of our standard Ca^{2+} sparks at three different source strengths, along with the corresponding amplitude distribution graphs, are shown in Fig. 5, *A* and *B*, respectively. As reported previously (Izu et al., 1998; Smith et al., 1998; Cheng et al.,

FIGURE 3 Inhibition of Ca^{2+} sparks by 5 μM RR. (*A*) Representative line scan fluorescence images of a permeabilized myocyte under control conditions and after addition to the "internal" solution 5 or 20 μM RR (as indicated above the images). Calibration bar: horizontal, 60 ms; vertical, 20 μm. The graphs below the images plot F/F_0 averaged over three spatial pixels centered at the brightest fluorescence events present in the corresponding images. (*B*) Surface plots of Ca^{2+} sparks under control conditions and in the presence of 5 μM RR. The signals were obtained by averaging 10 and 6 events for the control and presence of the drug, respectively. (*C*) Amplitude histograms for Ca^{2+} sparks recorded under control conditions and in the presence of RR. Data were from 393 and 77 events for control and RR, respectively, in four permeabilized cells. The data were corrected for missed events and distortions in the amplitude caused by noise using the correction functions presented in Fig. 1.

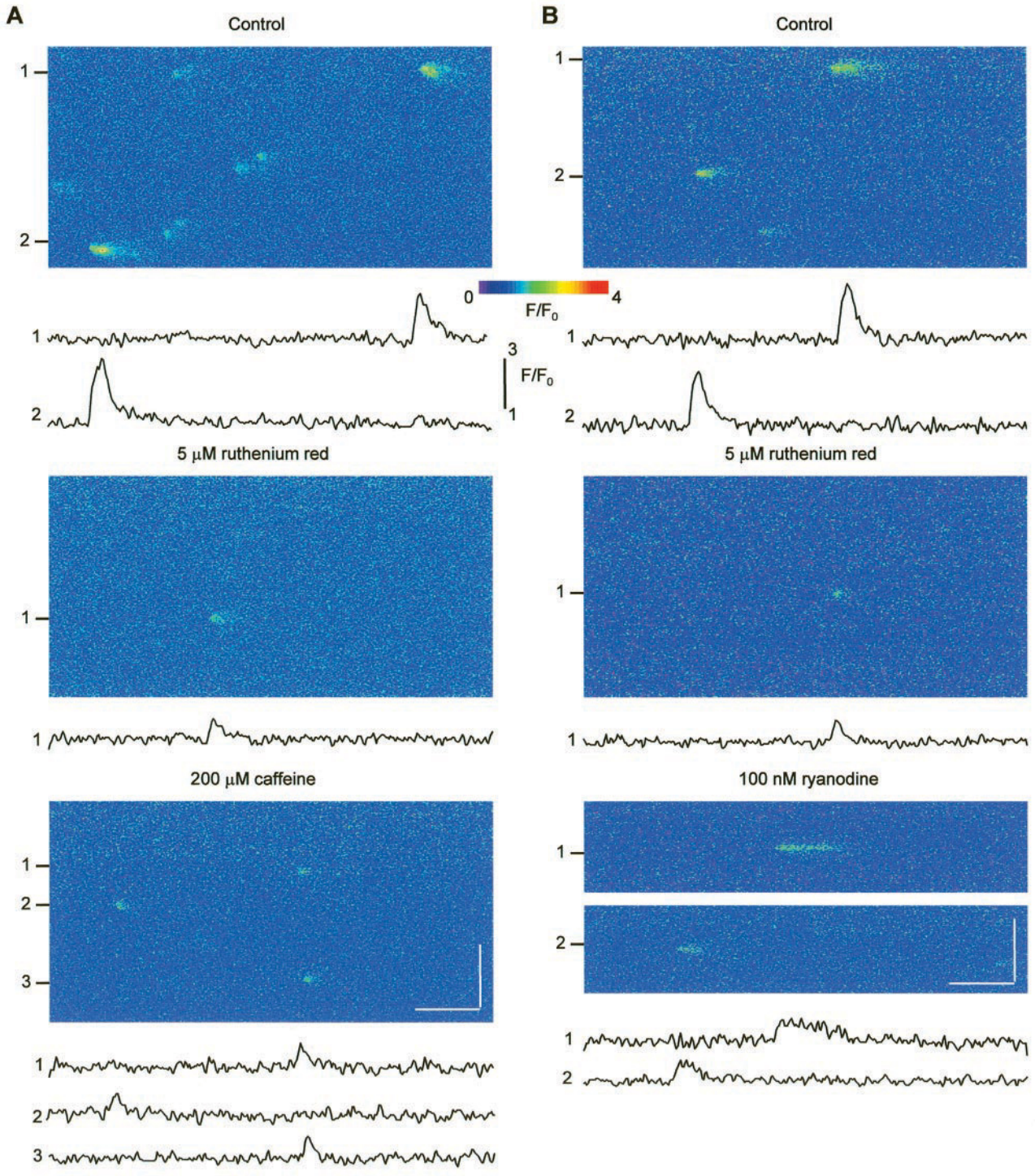

FIGURE 4 The effects of caffeine and ryanodine on the small fluorescence events in the presence of RR. (*A*) Representative line scan fluorescence images of Ca^{2+} release events under control conditions (*top panel*), 5 min after exposure of the cell to 5 μM RR (*middle panel*), and 30 s after introduction of 200 μM caffeine (*bottom panel*). The graphs plot F/F_0 averaged over three spatial pixels centered at Ca^{2+} release events. (*B*) Representative line scan fluorescence images of Ca^{2+} release events under control conditions (*top panel*), 4 min after exposure of the cell to 5 μM RR (*middle panel*), and 3 min after introduction of 100 nM ryanodine (*bottom panel*). The graphs plot F/F_0 averaged over three spatial pixels centered at Ca^{2+} release events. Calibration bars: horizontal, 100 ms; vertical, 20 μm.

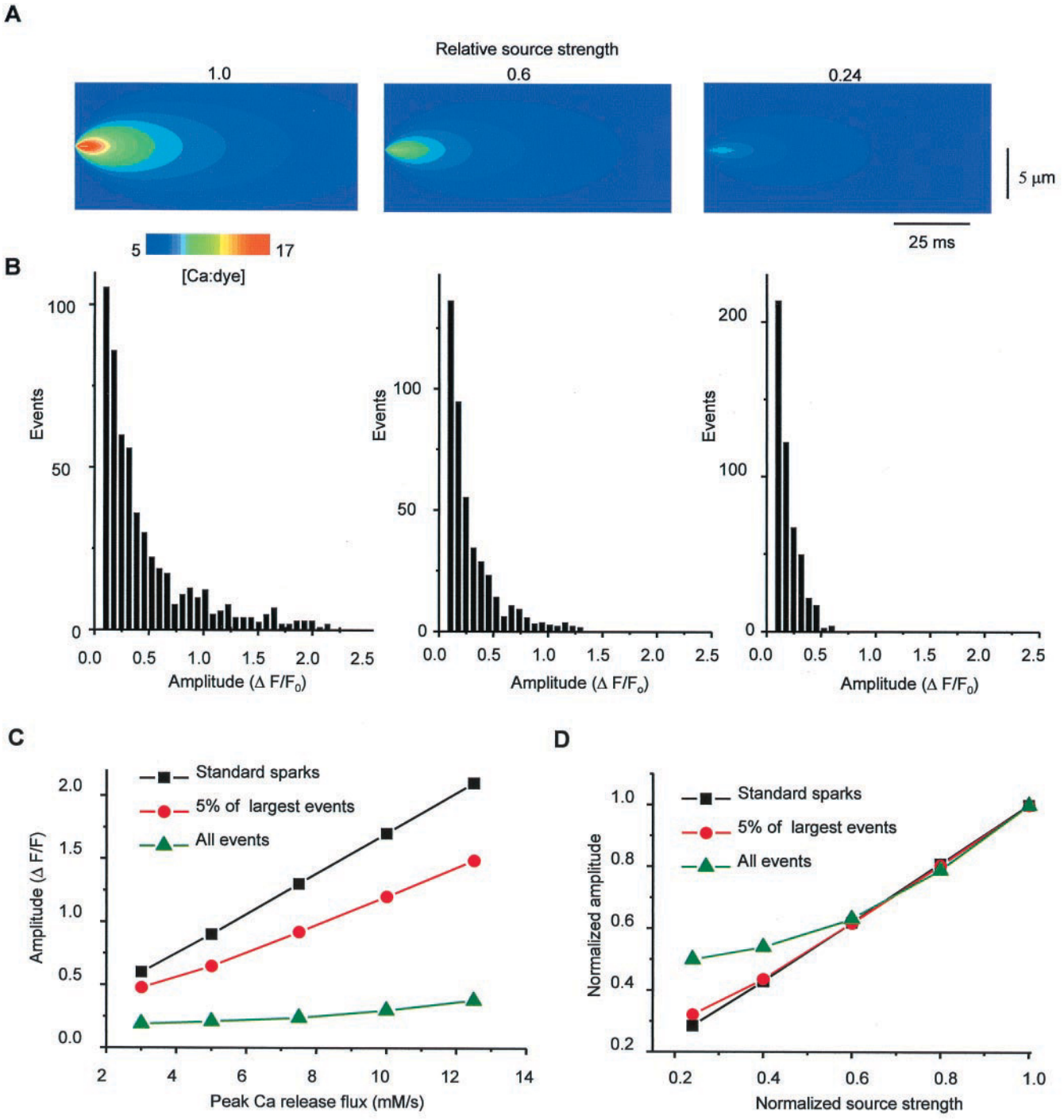

FIGURE 5 Effects of varying source strength on amplitude distribution of theoretical Ca^{2+} sparks. (*A*) Images of standard Ca^{2+} sparks simulated with underlying release fluxes of 10, 6, and 2.4 mM/s (relative source strengths 1.0, 0.6, and 0.24, respectively). (*B*) Theoretical amplitude histograms of events for the standard Ca^{2+} sparks presented in (*A*). (*C*) Relationship between the Ca^{2+} spark amplitude and underlying Ca^{2+} release flux determined for standard Ca^{2+} sparks (*squares*), the means of 5% of the largest sparks (*circles*), and the means of all the sparks in the amplitude distributions (*triangles*). (*D*) The same relationships as in (*C*) with normalized fluorescence amplitude and source strength values.

1999), the amplitude distribution of Ca^{2+} sparks decreases monotonically. Reducing source strength skews the distributions toward lower amplitudes.

Fig. 5 *C* plots the relationship between spark amplitude and underlying peak Ca^{2+} release flux for standard sparks (located at the center of the line scan) and for the cases of

5% of the brightest events and all events in the theoretical amplitude distributions. For standard Ca^{2+} sparks, the relationship is close to linear in the explored peak Ca^{2+} flux range. Inclusion of out-of-focus events shifts the graph to lower amplitudes, with notable distortion in linearity. These results are illustrated better in Fig. 5 *D*, in which both spark amplitudes and source strengths were normalized. It appears that the spark amplitude-source strength relationship obtained with the highest amplitude events is a reasonably good approximation of the same relationship for standard Ca^{2+} sparks. It can be deduced from these theoretical simulations that a 3-fold decrease in amplitude of brightest events is equivalent to an ~4-fold decrease in the peak release flux through the release units in the presence of RR.

Effects of RR on SR Ca^{2+} load

It has been shown previously that RyR inhibitors, including tetracaine and procaine, increase the SR Ca^{2+} load, presumably by reducing the leak of Ca^{2+} through the Ca^{2+} release channels (Stephenson and Wendt, 1986; Györke et al., 1997). Such changes in the amounts of releasable Ca^{2+} could result in underestimation of the degree of inhibition of SR Ca^{2+} release by the drug, and therefore require consideration. We used caffeine applications to assess the effects of RR on the SR Ca^{2+} content under the conditions of our experiments. Fig. 6 shows the effects of exposure of a permeabilized cell to 5 μM RR on Ca^{2+} transients elicited by application of 20 mM caffeine. The amplitude of the caffeine-induced Ca^{2+} transients was increased dramatically in the presence of the drug (0.299 $\pm$ 0.018 μM vs. 1.254 $\pm$ 0.344 μM). These series of experiments are summarized in Fig. 6 *B*, which plots the SR Ca^{2+} load before and after incubation of five different cells with 5 μM RR. The results are presented as changes in the total Ca^{2+} considering the amount of buffers (EGTA, Troponin-C) and the dye in the internal solution (see Eq. 2, Methods). It can be seen that the total amount of releasable Ca^{2+} increased by ~100% following incubation with RR (from 151 to 312 μmol/l cytosol).

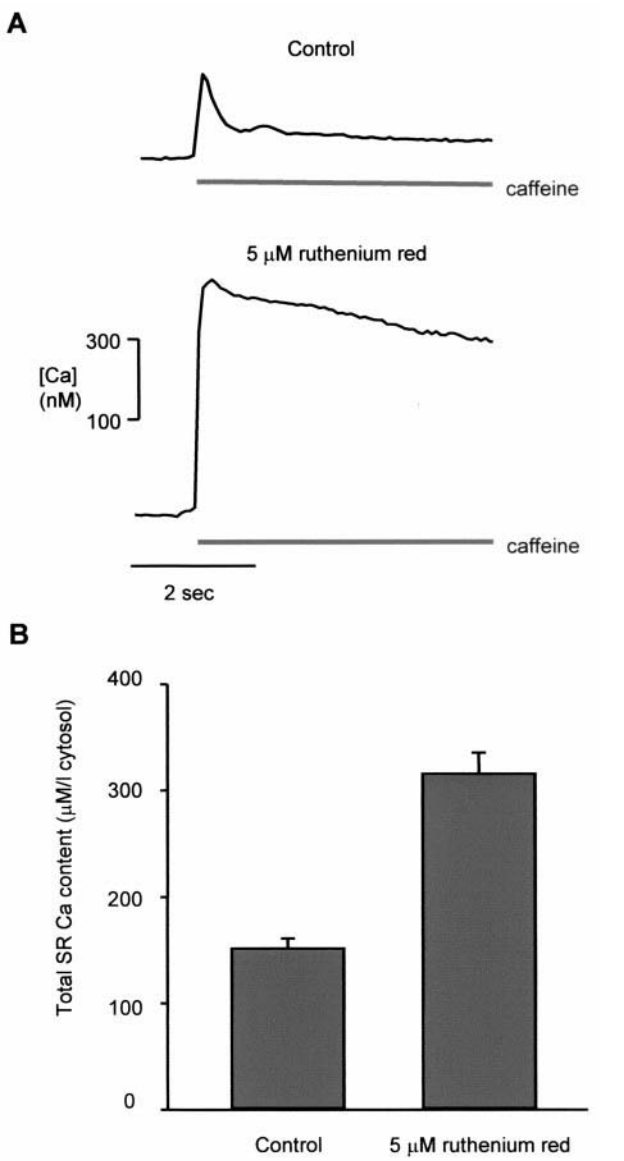

FIGURE 6 Effects of 5 μM RR on SR Ca^{2+} load. (*A*) Ca^{2+} transients induced by application of 20 mM caffeine to the whole bath under control conditions and in the presence of 5 μM RR. (*B*) Changes in the total SR Ca^{2+} content under the same conditions calculated by taking into account Ca^{2+} bound to EGTA, Troponin-C, and fluo-3, as described in the Methods section. Data are presented as mean $\pm$ SEM from five different experiments.

DISCUSSION

In this study we have compared the effects of the inhibitor of the Ca^{2+} release channels, RR, on single RyR channels in lipid bilayers and Ca^{2+} sparks in permeabilized rat ventricular myocytes. Our principal finding is that Ca^{2+} sparks can be reduced into smaller, "more elementary" fluorescence signals, implying that spark is a multi-channel event. We also showed that inhibition of Ca^{2+} sparks results in a dramatic increase in the SR Ca^{2+} content, suggesting that the resting SR Ca^{2+} load normally is limited not by Ca^{2+} uptake, but rather by leak of Ca^{2+} through RyRs.

Effects of RR on single-channel events and Ca^{2+} sparks

In bilayer experiments, RR at 5 μM inhibited P_o of RyRs by ~50-fold without significant effects on the conductance or the mean open time of the channel (Fig. 2; Table 1) These results are consistent with those from previous studies suggesting that RR inhibits RyRs primarily through reducing the overall availability of the channels by inducing long closures (Rousseau and Meissner, 1989; Ashley and Williams, 1990;

Lindsay and Williams, 1991; Xu et al., 1998). In permeabilized cardiac myocytes, RR at 5 μM reduced the frequency of Ca^{2+} release events by a lesser amount (~10-fold), and decreased the amplitude of the brightest events (with most probable localization on the line scan (Izu et al., 1998; present study) by ~3-fold (Fig. 3). The reduced inhibition in cells compared to that in lipid bilayers may be attributed to the elevation of intra-SR [Ca^{2+}] upon application of the drug in the permeabilized myocytes. We have shown previously that elevating lumenal Ca^{2+} can increase the open probability of reconstituted RyRs (Lukyanenko et al., 1996; Györke and Györke, 1998). Thus the inhibition of RyR activity by RR in permeabilized cells is partially offset by the potentiation of RyR activity due to elevated lumenal calcium. This is in contrast to the lipid bilayer experiments, where the calcium concentration in the compartment corresponding to the SR lumen (i.e., *trans* compartment) is fixed.

Ultrastructural evidence suggests that the volume scanned by the confocal microscope ($1 \times 1 \times 100$ μm) contains ~20,000 RyRs arranged in clusters composed of ~20 channels (Franzini-Armstrong and Protasi, 1997). If RR inhibits 95% of the channels, at any time it would leave ~1,000 RyR channels available for activation, i.e., one channel per cluster. Therefore, most events in the presence of RR are likely to represent openings of single RyRs in separate release units. It has been proposed that elementary release events associated with operation of single RyRs (i.e., "quarks"; Lipp and Niggli, 1996) are below the resolution of the confocal microscope. Under our experimental conditions we might be able to visualize these fundamental signals because of the increased SR Ca^{2+} load resulting in greater Ca^{2+} fluxes through the RyRs.

Recently, Xu and co-authors (1999) demonstrated that RR can induce gating to subconductance states in purified cardiac RyRs. In particular, they observed long-lived openings with conductance 25% of that of fully open channels recorded at 0 mV with 10 mM lumenal Ca^{2+} as the current carrier. In our bilayer experiments performed in native cardiac RyR channels, RR caused no formation of substates, nor did we observe prolonged fluorescence events that could be attributed to this type of gating behavior in permeabilized cells exposed to RR (although we were able to record fluorescence signals reflecting gating to substates induced by ryanodine, Fig. 4 *B*). These discrepancies in results could be ascribed to different experimental conditions (i.e., different RR concentrations, presence of MgATP in this but not in the referenced study) and to the possibility that the ability of RR to induce substates is different in purified versus native RyRs. Thus it is highly unlikely that our results are influenced by formation of substates among RyRs.

Effects of RR on SR Ca^{2+} load

Our estimate of the SR Ca^{2+} content (~151 μmol/l cytosol) under control conditions agrees well with previous estimates of the SR Ca^{2+} content in rat ventricular myocytes (185 μmol/l cytosol (Varro et al., 1993); 114 μmol/l cytosol (Bassani and Bers, 1995); 169 μmol/l cytoplasm (Diaz et al., 1997); 115 μmol/l cytosol (Terracciano and MacLeod, 1997)). Exposure of the cells to RR resulted in a dramatic increase in the SR Ca^{2+} content (to ~312 μmol/l cytosol). An analogous increase in the SR Ca^{2+} load has been observed previously in the presence of the local anesthetics tetracaine and procaine in cardiac myocytes exhibiting spontaneous and depolarization-induced Ca^{2+} release (Stephenson and Wendt, 1986; Györke et al., 1997; Overend et al., 1998). These effects have been attributed to inhibition by the drugs of Ca^{2+} leak through the SR Ca^{2+} release channels (Györke et al., 1997) or altered balance of Ca^{2+} fluxes mediated by the various cellular Ca^{2+} transport mechanisms during inhibition of periodically evoked induced Ca^{2+} release (Overend et al., 1998). In addition, the increased SR Ca^{2+} accumulation by local anesthetics could be due to the ability of these drugs to block the K^+ permeability of the SR membrane. It has been reported that various SR K^+ channel blockers, including procaine, can increase the amount of releasable Ca^{2+} in skinned amphibian muscle fibers (Fink and Stephenson, 1987; Fink and Veigel, 1996). The mechanism of action of these compounds on the SR Ca^{2+} content presumably involves indirect modulation of lumenal Ca^{2+} binding sites through altering counter-fluxes for H^+ and Mg^{2+} across the SR membrane (Fink and Stephenson, 1987; Fink and Veigel, 1996). Our present results obtained in quiescent permeabilized myocytes using RR, considered to be a more selective inhibitor of the RyR channels with no reported effects on the SR K^+ channels, demonstrate that inhibition of resting Ca^{2+} release through these channels can indeed cause a dramatic increase in the SR Ca^{2+} content.

The fact that inhibition of Ca^{2+} sparks can cause a more than twofold increase in the SR Ca^{2+} content indicates that resting Ca^{2+} leak via spontaneous openings of RyRs plays a significant role in setting the SR Ca^{2+} load in normal myocytes. Under resting conditions the SR Ca^{2+} load seems to be limited not by the ability of the Ca^{2+}-ATPase to move Ca^{2+} into the SR against the gradient, but rather by the dissipative loss of Ca^{2+} through the RyRs. An important implication of this result is that spark-mediated Ca^{2+} leak represents a potential site for regulation of the Ca^{2+} storing function of the SR. Indeed, influences enhancing basal RyR activity would be expected to lower the amount of Ca^{2+} sequestered, while agents that reduce RyR open probability would enhance SR Ca^{2+} accumulation, affecting the Ca^{2+} available for contractile activation (Lukyanenko and Györke, 2000).

How many RyRs are involved in Ca^{2+} spark generation?

The release flux underlying a spark is proportional to the product of the number of channels comprising a spark and

the magnitude of the single channel flux. The single channel flux in turn is a function of conductance, opening duration, and the Ca^{2+} gradient across the SR membrane. Therefore, the minimal number of channels contributing to a spark can be assessed from the reduction by the drug of the ensemble Ca^{2+} release flux underlying the spark, considering the elevation of $[Ca^{2+}]_{SR}$ in the presence of the drug and the possible effects of RR on the conductance and open state of single RyR channels.

In our experiments, RR (5 μM) reduced maximal spark amplitude by threefold (Fig. 3). This is due to a reduction in the number of channels participating in a spark, due to occlusion by RR. Theoretical studies of Ca^{2+} spark formation have shown that the amplitude of Ca^{2+} sparks is proportional to release flux underlying these local fluorescence events (Pratusevich and Balke, 1996; Smith et al., 1998). As we specifically estimated in the present study, a threefold reduction in the amplitude of the events corresponds to a fourfold inhibition of the underlying Ca^{2+} release flux (considering off-line sampling effects, Fig. 5).

By reducing efflux from the SR, RR effects an elevation in $[Ca^{2+}]_{SR}$. Thus the reduction in spark amplitude is partially mitigated by an increased concentration gradient between the SR lumen and the cytosol. In our experiments, the SR Ca^{2+} content increased from 151 to 312 μmol/l cytosol (Fig. 6). Assuming a lumenal Ca^{2+}-binding site concentration of 7 mM, $K_D \approx 0.5$ mM, and SR = 3.5% cell volume (Bers, 1991) this change in the total SR Ca^{2+} content would correspond to an increase in the free lumenal $[Ca^{2+}]$ from ~0.6 to 3 mM. These estimates are in the range provided by measurements of free intra-SR $[Ca^{2+}]$ using low Ca^{2+} affinity fluorescence indicators ($\geq$0.7 mM, Shannon and Bers, 1997) and NMR (from 1 to 5 mM, Chen et al., 1996) under normal loading conditions and under conditions of increased SR Ca^{2+} accumulation. Tinker and Williams (1992) reported a highly nonlinear relationship between efflux through RyRs and lumenal Ca^{2+} activity, one that saturated at 2–3 mM lumenal $[Ca^{2+}]$. According to their study, an increase in $[Ca^{2+}]_{SR}$ from 0.6 to 1 mM to 3 to 5 mM should result in at least a 2.5-fold increase in efflux through RyRs (the relationship is highly nonlinear saturating at 2–3 mM Ca^{2+}).

Ruthenium red at the concentrations used to suppress sparks in permeabilized cells induced long closures, but had no significant effects on conductance or mean open time of single RyRs in lipid bilayers (Fig. 2). Therefore, we rule out any significant alterations in spark amplitude due to alterations in single channel conductance or open-time duration.

Based on these results we conclude that Ca^{2+} sparks in the absence of the drug are generated by openings of at least $n \approx 4$ (decrease in ensemble Ca^{2+} flux) $\times$ 2.5 (increase in unidirectional Ca^{2+} flux through RyR) = 10 single RyR channels.

Our conclusion about the multi-channel nature of Ca^{2+} sparks is consistent with the low unitary Ca^{2+} conductance of reconstituted single RyR channels (Mejia-Alvarez et al., 1999) compared to the estimated Ca^{2+} release fluxes underlying Ca^{2+} sparks in both cardiac and skeletal muscle (Blatter et al., 1997; Rios et al., 1999). They also agree with the relatively low variance of mean amplitude of Ca^{2+} sparks recorded at fixed locations in mouse cardiac myocytes (Bridge et al., 1999).

This work was supported by National Institutes of Health Grants HL 52620 and HL 03739. S. Györke is an Established Investigator of the American Heart Association.

REFERENCES

Ashley, R. H., and A. J. Williams. 1990. Divalent cation activation and inhibition of single calcium release channels from sheep cardiac sarcoplasmic reticulum. *J. Gen. Physiol.* 95:981–1005.

Bassani, R. A., and D. M. Bers. 1995. Rate of diastolic Ca release from the sarcoplasmic reticulum of intact rabbit and rat ventricular myocytes. *Biophys. J.* 68:2015–2022.

Bassani, J. W., W. Yuan, and D. M. Bers. 1995. Fractional SR Ca release is regulated by trigger Ca and SR Ca content in cardiac myocytes. *Am. J. Physiol. Cell Physiol.* 268:C1313–C1319.

Baylor, S. M., W. K. Chandler, and M. W. Marshall. 1984. Calcium release and sarcoplasmic reticulum membrane potential in frog skeletal muscle fibres. *J. Physiol. (Lond.).* 348:209–238.

Bers, D. M. 1991. Excitation-contraction coupling and cardiac contractile force. Kluwer Academic Publishers, Dordrecht, The Netherlands.

Bers, D. M., and E. Perez-Reyes. 1999. Ca channels in cardiac myocytes: structure and function in Ca influx and intracellular Ca release. *Cardiovasc. Res.* 42:339–360.

Blatter, L. A., J. Huser, and E. Rios. 1997. Sarcoplasmic reticulum Ca^{2+} release flux underlying Ca^{2+} sparks in cardiac muscle. *Proc. Natl. Acad. Sci. USA.* 94:4176–4181.

Bridge, J. H., P. R. Ershler, and M. B. Cannell. 1999. Rapid report: properties of Ca^{2+} sparks evoked by action potentials in mouse ventricular myocytes. *J. Physiol. (Lond.).* 518:469–478.

Cannell, M. B., H. Cheng, and W. J. Lederer. 1994. Spatial non-uniformities in $[Ca^{2+}]_i$ during excitation-contraction coupling in cardiac myocytes. *Biophys. J.* 67:1942–1956.

Chen, W., C. Steenbergen, L. A. Levy, J. Vance, R. E. London, and E. Murphy. 1996. Measurement of free Ca^{2+} in sarcoplasmic reticulum in perfused rabbit heart loaded with 1,2-bis(2-amino-5,6-difluorophenoxy)ethane-*N*,*N*,*N*′,*N*′-tetraacetic acid by 19F NMR. *J. Biol. Chem.* 271:7398–7403.

Cheng, H., W. Lederer, and M. B. Cannell. 1993. Calcium sparks: elementary events underlying excitation-contraction coupling in heart muscle. *Science.* 262:740–744.

Cheng, H., M. R. Lederer, W. J. Lederer, and M. B. Cannell. 1996. Calcium sparks and $[Ca^{2+}]_i$ waves in cardiac myocytes. *Am. J. Physiol. Cell Physiol.* 270:C148–C159.

Cheng, H., L. S. Song, N. Shirokova, A. Gonzalez, E. G. Lakatta, E. Rios, and M. D. Stern. 1999. Amplitude distribution of calcium sparks in confocal images: theory and studies with an automatic detection method. *Biophys. J.* 76:606–617.

Dettbarn, C. A., R. Betto, G. Salviati, P. Palade, G. M. Jenkins, and R. A. Sabbadini. 1994. Modulation of cardiac sarcoplasmic reticulum ryanodine receptor by sphingosine. *J. Mol. Cell Cardiol.* 26:229–242.

Diaz, M. E., A. W. Trafford, S. C. O'Neill, and D. A. Eisner. 1997. Measurement of sarcoplasmic reticulum Ca^{2+} content and sarcolemmal Ca^{2+} fluxes in isolated rat ventricular myocytes during spontaneous Ca^{2+} release. *J. Physiol. (Lond.).* 501:3–16.

Eisner, D. A., A. W. Trafford, M. E. Diaz, C. L. Overend, and S. C. O'Neill. 1998. The control of Ca release from the cardiac sarcoplasmic

reticulum: regulation versus autoregulation. *Cardiovasc. Res.* 38: 589–604.

Fink, R. H. A., and D. G. Stephenson. 1987. Ca^{2+}-movements in muscle modulated by the state of K^{+}-channels in the sarcoplasmic reticulum membranes. *Pfluegers Arch.* 409:374–380.

Fink, R. H. A., and C. Veigel. 1996. Calcium uptake and release modulated by counter-ion conductances in the sarcoplasmic reticulum of skeletal muscle. *Acta Physiol. Scand.* 156:387–396.

Franzini-Armstrong, C., and F. Protasi. 1997. Ryanodine receptors of striated muscles: a complex channel capable of multiple interactions. *Physiol. Rev.* 77:699–729.

Gillespie, D. T. 1976. A general method of numerically simulating the stochastic time evolution of coupled chemical reactions. *J. Comp. Phys.* 22:403–434.

Györke, I., and S. Györke. 1998. Regulation of the cardiac ryanodine receptor channel by luminal Ca^{2+} involves luminal Ca^{2+} sensing sites. *Biophys. J.* 75:2801–2810.

Györke, S., V. Lukyanenko, and I. Györke. 1997. Dual effects of tetracaine on spontaneous calcium release in rat ventricular myocytes. *J. Physiol. (Lond.).* 500:297–309.

Izu, L. T., W. G. Wier, and C. W. Balke. 1998. Theoretical analysis of the Ca^{2+} spark amplitude distribution. *Biophys. J.* 75:1144–1162.

Kawai, M., and M. Konishi. 1994. Measurement of sarcoplasmic reticulum calcium content in skinned mammalian cardiac muscle. *Cell Calcium.* 16:123–136.

Langer, G. A., and A. Peskoff. 1996. Calcium concentration and movement in the diadic cleft space of the cardiac ventricular cell. *Biophys. J.* 70:1169–1182.

Lindsay, A. R., and A. J. Williams. 1991. Functional characterisation of the ryanodine receptor purified from sheep cardiac muscle sarcoplasmic reticulum. *Biochim. Biophys. Acta.* 1064:89–102.

Lipp, P., and E. Niggli. 1996. Submicroscopic calcium signals as fundamental events of excitation-contraction coupling in guinea-pig cardiac myocytes. *J. Physiol. (Lond.).* 492:31–38.

Lopez-Lopez, J. R., P. S. Shacklock, C. W. Balke, and W. G. Wier. 1995. Local calcium transients triggered by single L-type calcium channel currents in cardiac cells. *Science* 268:1042–1045.

Lukyanenko, V., and S. Györke. 1999. Ca^{2+} sparks and Ca^{2+} waves in saponin-permeabilized cardiac myocytes. *J. Physiol. (Lond.).* 521: 575–585.

Lukyanenko, V., and S. Györke. 2000. Dynamic regulation of SR Ca content by lumenal Ca-sensitive leak through RyRs in rat cardiomyocytes. *Biophys. J.* 78:440*a*. (Abstr).

Lukyanenko, V., I. Györke, and S. Györke. 1996. Regulation of calcium release by calcium inside the sarcoplasmic reticulum in ventricular myocytes. *Pfluegers Arch.* 432:1047–1054.

Lukyanenko, V., S. Subramanian, I. Györke, T. Wiesner, and S. Györke. 1999. The role of sarcoplasmic reticulum luminal Ca^{2+} in generation of Ca^{2+} wave in rat ventricular myocytes. *J. Physiol. (Lond.).* 518: 173–186.

Lukyanenko, V., T. F. Wiesner, and S. Györke. 1998. Termination of Ca^{2+} release during Ca^{2+} sparks in rat ventricular myocytes. *J. Gen. Physiol.* 507:667–677.

Meissner, G. 1994. Ryanodine receptor/Ca^{2+} release channels and their regulation by endogenous effectors. *Annu. Rev. Physiol.* 56:485–508.

Mejia-Alvarez, R., C. Kettlun, E. Rios, M. Stern, and M. Fill. 1999. Unitary Ca^{2+} current through cardiac ryanodine receptor channels under quasi-physiological ionic conditions. *J. Gen. Physiol.* 113:177–186.

Overend, C. L., S. C. O'Neill, and D. A. Eisner. 1998. The effect of tetracaine on stimulated contractions, sarcoplasmic reticulum Ca^{2+} content and membrane current in isolated rat ventricular myocytes. *J. Physiol. (Lond.).* 507:759–769.

Pratusevich, V. R., and C. W. Balke. 1996. Factors shaping the confocal image of the calcium spark in cardiac muscle cells. *Biophys. J.* 71: 2942–2957.

Rios, E., M. D. Stern, A. Gonzalez, G. Pizarro, and N. Shirokova. 1999. Calcium release flux underlying Ca^{2+} sparks of frog skeletal muscle. *J. Gen. Physiol.* 114:31–48.

Rousseau, E., and G. Meissner. 1989. Single cardiac sarcoplasmic reticulum Ca^{2+}-release channel: activation by caffeine. *Am. J. Physiol. Heart Circ. Physiol.* 256:H328–H333.

Shannon, T. R., and D. M. Bers. 1997. Assessment of intra-SR free [Ca] and buffering in rat heart. *Biophys. J.* 73:1524–1531.

Smith, G. D., J. E. Keizer, M. D. Stern, W. J. Lederer, and H. Cheng. 1998. A simple numerical model of calcium spark formation and detection in cardiac myocytes. *Biophys. J.* 75:15–32.

Song, L. S., M. D. Stern, E. G. Lakatta, and H. Cheng. 1997. Partial depletion of sarcoplasmic reticulum calcium does not prevent calcium sparks in rat ventricular myocytes. *J. Physiol. (Lond.).* 505:665–675.

Stephenson, D. G., and I. R. Wendt. 1986. Effects of procaine on calcium accumulation by the sarcoplasmic reticulum of mechanically disrupted rat cardiac myocytes. *J. Physiol. (Lond.).* 373:195–207.

Terracciano, C. M., and K. T. MacLeod. 1997. Measurements of Ca^{2+} entry and sarcoplasmic reticulum Ca^{2+} content during the cardiac cycle in guinea pig and rat ventricular myocytes. *Biophys. J.* 72:1319–1326.

Tinker, A., and A. J. Williams. 1992. Divalent cation conduction in the ryanodine receptor channel of sheep cardiac muscle sarcoplasmic reticulum. *J. Gen. Physiol.* 100:479–493.

Varro, A., N. Negretti, S. B. Hester, and D. A. Eisner. 1993. An estimate of the calcium content of the sarcoplasmic reticulum in rat ventricular myocytes. *Pfluegers Arch.* 423:158–160.

Xiao, R. P., H. H. Valdivia, K. Bogdanov, C. Valdivia, E. G. Lakatta, and H. Cheng. 1997. The immunophilin FK506-binding protein modulates Ca^{2+} release channel closure in rat heart. *J. Physiol. (Lond.).* 500: 343–354.

Xu, L., A. Tripathy, D. A. Pasek, and G. Meissner. 1998. Potential for pharmacology of ryanodine receptor/calcium release channels. *Ann. NY Acad. Sci.* 853:130–148.

Xu, L., A. Tripathy, D. A. Pasek, and G. Meissner. 1999. RR modifies the cardiac and skeletal muscle Ca(2+) release channels (ryanodine receptors) by multiple mechanisms. *J. Biol. Chem.* 274:32680–32691.